1116 *KSME International Journal, Vol. 12, No. 6, pp. 1116~1125, 1998*

Diving Autopilot Design for Underwater Vehicles Using Multi-Objective Control Synthesis

Sam-Sang You* and Young-Ho Chai**

(Received February 23, 1998)

This paper presents the mathematical modeling, guidance and robust control synthesis of a highly maneuverable submersible vehicle (or underwater vehicle) when performing a specific mission at shallow submergence conditions. First, the vertical plane motions (heave and pitch) of the vehicle are modeled by a set of maneuvering equations. After model simplification, a state-space model is compactly obtained. Then a state-feedback controller is proposed for the accurate depth-keeping and pitch motion controls of the vehicle. The control actions to the generalized plant can be provided by the mixed H_2/H_∞ optimal synthesis as well as closed-loop pole constraint with LMIs. The feasibility of the guidance and control approach is verified with direct numerical simulations. The proposed approach ensures reasonable depth-keeping and minimal pitch motions, even under a given uncertainty condition.

Key Words: Underwater Vehicle, Diving (Vertical) Plane, State-Space Model, Disturbance, Autopilot, Mixed H_2/H_∞ Synthesis, Pole Constraint, Linear Matrix Inequalities (LMIs).

Nomenclature

$\boldsymbol{I}_n, \boldsymbol{0}_{n\times m}$: $n\times n$ identity matrix, nxm null matrix

$\Re^+$: set of positive real numbers in $[0, \infty]$ with real field $\Re$

$\boldsymbol{A}, \boldsymbol{B}$: system matrix, (control or disturbance) input matrix

$\boldsymbol{C}, \boldsymbol{D}$: output matrix, (control or disturbance) input matrix

$\boldsymbol{J}_{\bar{y}}$: pitch moment of inertia about $\bar{y}$-body axis

U : surge rate (forward speed) along with the axis $\bar{x}$

ω : heave rate (vertical speed) along with the axis $\bar{z}$

θ, q : pitch angle, pitch angular velocity

$\boldsymbol{y}$: measured output vector

$(\bar{x}_B, \bar{z}_B)$: coordinates of the center of buoyancy in the body frame

$(\bar{x}_G, \bar{z}_G)$: coordinates of the c. g. in the body frame

m_v, W_B, W_W : vehicle mass, buoyancy, weight

ρ : fluid density

$\boldsymbol{z}_\infty, \boldsymbol{z}_2$: vectors of performance outputs of interest

$\boldsymbol{A}>\boldsymbol{0}(\boldsymbol{A}<\boldsymbol{0})$: positive-definite (negative-definite) matrix

$\left[\begin{array}{c|c}\boldsymbol{A} & \boldsymbol{B}\\ \hline \boldsymbol{C} & \boldsymbol{D}\end{array}\right]$: state-space realization of the transfer matrix $\boldsymbol{C}(\boldsymbol{s}(\boldsymbol{I}-\boldsymbol{A})^{-1}\boldsymbol{B}+\boldsymbol{D}$

$\bar{\omega}$: angular frequency

$\|\boldsymbol{w}\|_2=(\int_0^\infty \boldsymbol{w}^T\boldsymbol{w}dt)^{1/2}<\infty$: the L_2(energy) norm of the vector of signals $\boldsymbol{w}(t)$

$\|\boldsymbol{A}(s)\|_\infty=\sup_{0<\bar{\omega}<\infty}\bar{\sigma}[\boldsymbol{A}(j\bar{\omega})]$: H_∞ norm of the stable transfer function matrix $\boldsymbol{A}(s)$

$\|\boldsymbol{A}(s)\|_2=\{(1/2\pi)\int_{-\infty}^{\infty} Trace[\boldsymbol{A}^*(j\bar{\omega})\boldsymbol{A}(j\bar{\omega})$

* Assistant Professor, School of Mechanical Systems Engineering, Korea Maritime University, Pusan, Korea

** Assistant Professor, Department of Mechanical Engineering Chung-Ang University, Seoul, Korea

$d\bar{\omega}]\}^{1/2}$: H_2 norm of the matrix $A(s)$

$\bar{\sigma}(A)$: largest (or maximum) singular value of A

$(\tilde{\sigma})$: normalized version of variable (σ)

1. Introduction

Research on submersible vehicle is a field of increasing interest due to its many applications. Especially the high-performance vehicles are expected to provide increased maneuverability and agility at various speeds as well as depths. The design of accurate maneuvering controller, commonly called autopilot for underwater vehicle, is challenging because the system dynamics are highly nonlinear in nature and contains various uncertainties. In fact, a vehicle performing a specific mission near the sea surface is subject to external perturbations caused by sea conditions such as underwater currents and waves. Therefore, the vehicle autopilot must be capable of exhibiting considerable robustness to all disturbance effects and keeping the vehicle in the desired depth.

Various design methodologies have been developed over the past decades for dynamics, control synthesis, and stability analysis of submersible vehicle (Geuler, 1989; Healey and Lienard, 1993; Papoulias, 1993) in which the PID-type and optimal controllers are widely used in calm sea conditions. In order to improve the autopilot's performance, multivariable methods have been applied to the depth-keeping control of modern submarines (Marshfield 1991). Earlier works in multivariable control synthesis have mainly utilized a quadratic cost function to minimize the 2-norm of a system response to white noise inputs. As shown in references (Bernstein *et al.*, 1991; Doyle et al., 1989), the linear quadratic Guassian (LQG) type of cost function is often a practical criterion for minimizing tracking errors or control signal variations. Eventhough, the H_2 approach is well suited to many real systems, it is well known that its stability and performance cannot be guaranteed in the presence of various uncertainties. As is in case of any submersible vehicles, the system is expected to operate in a highly variable environment and will be effected by some fluctuations at shallow depth. One of the most important advances in the past decades on the multivariable control is the development of H_∞ control theory (Glover and Doyle, 1988). It has been recognized that the H_∞ synthesis guarantees the robust stability and disturbance rejection performance in the presence of uncertainty, but that the H_∞ -optimal controller typically leads to an intolerably large control effort. The mixed H_2 and H_∞ performance criteria become indispensable to quantitatively demonstrate design tradeoffs. Several researchers have devoted considerable attention over the past several years to the mixed H_2/H_∞ control method for uncertain dynamical systems (Bernstein *et al.*, 1991; Rotea and Khargonekar, 1992). On the other hand, it must be noted that many control problems can be cast into multi-objective characteristics and readily solved by LMI approach (Boyd *et al.*, 1994). In addition, several authors (Iwasaki and Skelton, 1994; Chilali and Gahinet, 1996) have shown that an LMI synthesis is useful tool for multiobjective control problems.

To the author's knowledge, there has been no paper considering the comprehensive dynamics issues as well as the LMI-based H_2/H_∞ control approach for submersible vehicles. This study is to design the vehicle autopilot for vertical plane motions via LMIs: H_2 optimal with H_∞ disturbance attenuation and closed-loop pole placement. As a result, the submersible vehicle maintains a nearly constant depth relative to the sea surface and has minimal angular pitch motions as well in the presence of the uncertainties.

The paper is organized as follows. Sec 2 describes the linear vertical dynamics of the vehicle. In Sec 3, we present a class of robust linear controllers for the pitch/depth maneuver. In Sec 4, the autopilot performance has been extensively assessed through a series of numerical simulations. Finally, the contributions and conclusions of the work are summarized in Section 5.

2. Underwater Vehicle Modelling

2.1 Vehicle kinematics and dynamics

The standard submersible vehicle being considered in the study is a realistic one but does not represent any particular model in use. For most submersible vehicles the motion analysis is conventionally separated into motions in the vertical plane and horizontal plane.

Figure 1 depicts two orthonormal coordinate systems for the diving plane; $(\overline{O}-\overline{X}, \overline{Y}, \overline{Z})$ is the inertial reference frame fixed on sea surface with $\overline{Z}$ pointing "down"; $(\bar{o}-\bar{x}, \bar{y}, \bar{z})$ is the body-fixed frame with its origin located at the vehicle's center of gravity (or c. g.). As is usual, the diving (or depth/pitch) plane guidance and control surfaces include a set of hydroplanes: bow hydroplane angle (δ_b), stern hydroplane (δ_s).

In the vehicle linearization procedure, typical coefficients in the Taylor series expansion take the forms of partial derivatives of forces or moments terms. For example, the stability derivative coefficients Z_q and M_q respectively represent the shorthand notations of

$$Z_q \equiv \left[\frac{\partial Z}{\partial q}\right]_{q_0} \text{ and } M_q \equiv \left[\frac{\partial M}{\partial q}\right]_{q_0}$$

which mean that the partial motion derivatives of the heaving force Z and the pitch moment M with respect to pitch rate q taken at the steady-state reference point (q_0). Considering only the diving plane motions with constant forward speed (U), the coupled differential equations for vehicle motions are written in the body frame as follows (Geuler, 1989; Healey and Lienard, 1993; Marshfield, 1991; Papoulias, 1993):

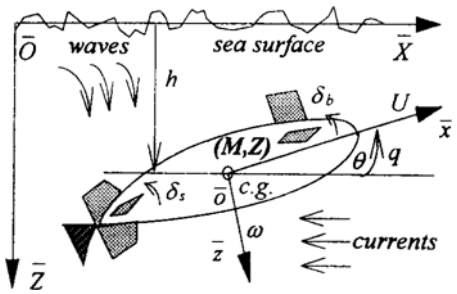

Fig. 1 Submarine system configuration (lateral view).

(Heave Motion): $m_v(\dot{\omega}-Uq-\bar{x}_G\dot{q}) =$

$$\frac{\rho}{2}l^2[Z_\omega U\omega + U^2(Z_{\delta_b}\delta_b + Z_{\delta_s}\delta_s)] + \frac{\rho}{2}l^3(Z_q Uq + Z_{\dot{\omega}}\dot{\omega}) + \frac{\rho}{2}l^4 Z_{\dot{q}}\dot{q} + (W_W - W_B)\cos\theta + g_F \quad (1)$$

(Pitch Motion): $I_{\bar{y}}\dot{q} - m_v[\bar{x}_G(\dot{\omega}-Uq)] =$

$$\frac{\rho}{2}l^3[M_\omega U\omega + U^2(M_{\delta_b}\delta_b + M_{\delta_s}\delta_s)] + \frac{\rho}{2}l^4(M_q Uq + M_{\dot{\omega}}\dot{\omega}) + \frac{\rho}{2}l^5 M_{\dot{q}}\dot{q} - (\bar{x}_G W_W - \bar{x}_B W_B)\cos\theta - (\bar{z}_G W_W - \bar{z}_B W_B)\sin\theta + g_M \quad (2)$$

The expressions on the right-hand sides in (1-2) represent the hydrodynamic and external heave forces and the corresponding pitch moments acting on the vehicle; they refer to hull, weight and buoyancy, hydroplanes, drag, and other external efforts. In the above formulation, we ignore the higher-order derivatives terms in the Taylor expansion. The numerical values of any particular Taylor coefficients in (1-2) depend on a specific vehicle model. In general, the coefficients, which are dimensionless derivative constants, are calculated by means of experimental tests for a prototype model (Clayton and Bishop, 1982). When an underwater vehicle is operating in a shallow submerged condition, the major external forces (moments) include the sea surface disturbance, the current, wave, and other external efforts. In order to avoid complex mathematics, it is assumed that the forces and moments due to the various sea conditions change slowly. They can be represented by first-order polynomial forms $g_F = b_1 w_1$ and $g_M = b_2 w_2$ (You, 1996) with $b_i \in \Re^+$. Now the kinematic relations are governed by the following equations, which determine the c. g. path relative to the inertial reference frame:

$$\dot{\theta} = q \quad (3)$$

$$\dot{h} = \omega\cos\theta - U\sin\theta + \omega\cos\theta \approx \omega - U\theta \quad (4)$$

where the pitch angle θ is small $(\theta \approx 0)$, namely $\sin(\theta) \approx \theta$ and $\cos(\theta) \approx 1$. Without loss of generality, the following assumptions are made to develop the state-space equations of motion:

[A1]: The rudders are locked for the pitch plane

[A2]: The vehicle is a rigid with having a port/

starport symmetric structure.

[A3]: The metacentric height $\bar{z}_{GB}(=\bar{z}_G-\bar{z}_B>0)$ is equal to $\bar{z}_G$ with $\bar{z}_B=0$

[A4]: The vehicle is neutrally buoyant, or $W_W=W_B$

[A5]: The body $\bar{x}$-frame of c. g. is equal to that of buoyancy, or $\bar{x}_G=\bar{x}_B$

2.2 State-space model of the vehicle motion

For the compact dynamic and kinematic model, we define the state-vector as $\boldsymbol{x}=[\delta\omega,\ \delta q,\ \delta h,\ \delta\theta]^T$, the control input variables as $\boldsymbol{u}=[\delta_b,\ \delta_s]^T$, and the uncertainty (or disturbance) vector as $\boldsymbol{w}=[w_1,\ w_2]^T$. Based on the above assumptions, the linearized form of the vehicle model (1-4) about the operating points $\boldsymbol{x}_0$ can be expressed as:

$$\boldsymbol{E}_M\dot{\boldsymbol{x}}=\boldsymbol{E}_A\boldsymbol{x}+\boldsymbol{E}_{B_1}\boldsymbol{\omega}+\boldsymbol{E}_{B_2}\boldsymbol{u} \tag{5}$$

A set of matrices in (5) can be written as:

$$\boldsymbol{E}_M=\begin{bmatrix} m_v-\mu_2Z_{\dot\omega} & -(m_v\bar{x}_G+\mu_3Z_{\dot q}) & 0 & 0\\ -(m_v\bar{x}_G+\mu_3M_{\dot\omega} & J_{\bar y}-\mu_4M_{\dot q} & 0 & 0\\ 0 & 0 & 1 & 0\\ 0 & 0 & 0 & 1\end{bmatrix},$$

$$\boldsymbol{E}_A=\begin{bmatrix} \mu_1Z_\omega U & (m_v+\mu_2Z_q)\,U & 0 & 0\\ \mu_3M_\omega U & -(m_v\bar{x}_G-\mu_3M_q)\,U & 0 & 0\\ 1 & 0 & 0 & 0\\ 0 & 1 & 0 & 0\end{bmatrix},$$

$$\boldsymbol{E}_{B_1}=\begin{bmatrix} b_1 & 0\\ 0 & b_2\\ 0 & 0\\ 0 & 0\end{bmatrix},\quad \boldsymbol{E}_{B_2}=\begin{bmatrix} \mu_1Z_{\delta_b}U^2 & \mu_1Z_{\delta_s}U^2\\ \mu_2M_{\delta_b}U^2 & \mu_2M_{\delta_s}U^2\\ 0 & 0\\ 0 & 0\end{bmatrix}$$

where $\mu_1=(\rho/2)\,l^2$; $\mu_2=(\rho/2)\,l^3$; $\mu_3=(\rho/2)\,l^4$; $\mu_4=(\rho/2)\,l^5$. Note that the state variables $\delta\omega$, δq, δh and $\delta\theta$ in (5) are variations from the steady-state operating points ($\boldsymbol{x}_0=\boldsymbol{0}$); $\delta\omega\equiv\omega_0-\omega$, $\delta q\equiv q_0-q$, $\delta h\equiv h_0-h$, and $\delta\theta\equiv\theta_0-\theta$. Referring to the model given in descriptor form (5), we obtain the state-space realization as

$$\dot{\boldsymbol{x}}=\boldsymbol{A}\boldsymbol{x}+\boldsymbol{B}_1\boldsymbol{w}+\boldsymbol{B}_2\boldsymbol{u} \tag{6}$$

where a set of matrices are denoted by $\boldsymbol{A}=\boldsymbol{E}_M^{-1}\boldsymbol{E}_A$, $\boldsymbol{B}_1=\boldsymbol{E}_M^{-1}\boldsymbol{E}_{B_1}$, and $\boldsymbol{B}_2=\boldsymbol{E}_M^{-1}\boldsymbol{E}_{B_2}$ with $\det(\boldsymbol{E}_M)\neq0$. For an accurate pitch/depth maneuver, the vehicle autopilot controller must compensate the uncertainty effects ($\boldsymbol{w}$) and keep the vehicle in the desired depth with a minimal pitch angular motion.

3. Vehicle Control Synthesis with LMIs

3.1 Control formulation with state-feedback

The design of robust autopilot for submersible vehicles generally involves many constraints and competing objectives. In the paper, an autopilot is required to minimize depth and pitch angular fluctuations with appropriate control energy. Consider the general mixed-norm synthesis for multiple objective problems shown in Fig. 2. First, the generalized plant $\boldsymbol{P}$(or $\sum_P$) to be controlled by the gain matrix $\boldsymbol{K}(\in\boldsymbol{k})$ is given by the state-space realization with assuming full measurements of its state vector:

$$\sum_P\begin{cases}\dot{\boldsymbol{x}}=\boldsymbol{A}\boldsymbol{x}+\boldsymbol{B}_1\boldsymbol{w}+\boldsymbol{B}_2\boldsymbol{u}\\ \boldsymbol{z}_\infty=\boldsymbol{C}_1\boldsymbol{x}+\boldsymbol{D}_{11}\boldsymbol{w}+\boldsymbol{D}_{12}\boldsymbol{u}\\ \boldsymbol{z}_2=\boldsymbol{C}_2\boldsymbol{x}+\boldsymbol{D}_{21}\boldsymbol{w}+\boldsymbol{D}_{22}\boldsymbol{u}\\ \boldsymbol{y}=\boldsymbol{x}\end{cases} \tag{7}$$

with a control law $\boldsymbol{u}=\boldsymbol{K}\boldsymbol{x}$

where $\boldsymbol{A}$, $\boldsymbol{B}_1$, $\boldsymbol{B}_2$, $\boldsymbol{C}_1$, $\boldsymbol{C}_2$, $\boldsymbol{D}_{11}$, $\boldsymbol{D}_{12}$, $\boldsymbol{D}_{21}$ and $\boldsymbol{D}_{22}$ are real matrices of compatible dimensions; $\boldsymbol{k}$ denotes the set of all real proper controllers. Then the augmented plant is compactly rewritten as

$$\boldsymbol{P}=\left[\begin{array}{c|cc} \boldsymbol{A} & \boldsymbol{B}_1 & \boldsymbol{B}_2\\ \hline \boldsymbol{C}_1 & \boldsymbol{D}_{11} & \boldsymbol{D}_{12}\\ \boldsymbol{C}_2 & \boldsymbol{D}_{21} & \boldsymbol{D}_{22}\\ \boldsymbol{I} & \boldsymbol{0} & \boldsymbol{0}\end{array}\right] \tag{8}$$

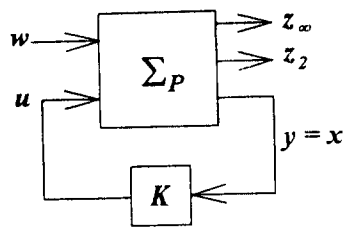

Fig. 2 The multi-objective framework with state-feedback regulator.

Moreover, the state-space realizations of the closed-loop systems are described by

$$\Sigma_{cl}: \begin{bmatrix} \dot{x}_{cl} \\ z_\infty \\ z_2 \end{bmatrix} = \begin{bmatrix} A_{cl} & B_{cl} \\ C_{cl\infty} & D_{cl\infty} \\ C_{cl2} & D_{cl2} \end{bmatrix} \begin{bmatrix} x_{cl} \\ w \end{bmatrix} \tag{9}$$

where the closed-loop matrices with x_{cl} have appropriate sizes and are further given as

$$\begin{bmatrix} A_{cl} & B_{cl} \\ C_{cl\infty} & D_{cl\infty} \\ C_{cl2} & D_{cl2} \end{bmatrix} = \begin{bmatrix} A+B_2K & B_1 \\ C_1+D_{12}K & D_{11} \\ C_2+D_{22}K & D_{21} \end{bmatrix} \tag{10}$$

Let $\Sigma_{cl\infty}=\{A_{cl}, B_{cl}, C_{cl\infty}, D_{cl\infty}\}$ and $\Sigma_{cl2}=\{A_{cl}, B_{cl}, C_{cl2}, D_{cl2}\}$ denote the state-space realizations of $T_{z_\infty w}$ and $T_{z_2 w}$, respectively. In the autopilot synthesis, the maps $T_{z_\infty w}$ and $T_{z_2 w}$ represent the closed-loop matrices from the inputs w to the controlled performance outputs z_∞ and z_2, respectively. Then the closed-loop transfer matrix leading to the lower linear fractional transformation (LFT) of P and K (Bernstein et al., 1991), if well posed, is defined as

$$T_{z_\infty w} = \left[\begin{array}{c|c} A_{cl} & B_{cl} \\ \hline C_{cl\infty} & D_{cl\infty} \end{array}\right] = \left[\begin{array}{c|c} A+B_2K & B_1 \\ \hline C_1+D_{12}K & D_{11} \end{array}\right] \tag{11}$$

$$T_{z_2 w} = \left[\begin{array}{c|c} A_{cl} & B_{cl} \\ \hline C_{cl2} & D_{cl2} \end{array}\right] = \left[\begin{array}{c|c} A+B_2K & B_1 \\ \hline C_2+D_{22}K & D_{21} \end{array}\right] \tag{12}$$

With these notations and assumptions in mind, we are interested in synthesizing the vehicle autopilot controller.

Problem Statement: Given the vehicle plant P with a predetermined scalar $\gamma_\infty>0$, find a stabilizing controller K for all admissible uncertainties w to solve the following synthesis problem via LMI optimization (Khargonekar and Rotea, 1991; Bernstein *et al.*, 1991):

$$\inf_{K \text{ stabilizing}} \|T_{z_2 w}\|_2 = \gamma_{2opt} \text{ subject to } \|T_{z_\infty w}\|_\infty < \gamma_\infty$$

with a closed-loop pole constraint in a desired region Π_{cl}.

In the above statement, the set Π_{cl} is a subset of complex left-half plane.

3.2 Pole assignment in the prescribed region

As specified in Fig. 3, the closed-loop poles are placed in a subregion $\Pi_{cl}(\alpha, \beta, r)$ of open left-half plane with a closed-loop pole $\chi_i \in \Pi_{cl}$:

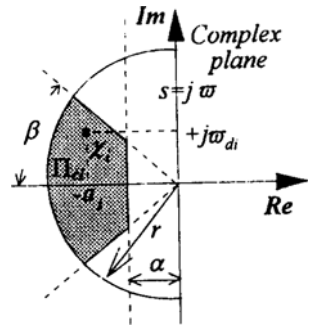

Fig. 3 Regional set Π_{cl} for an arbitrary closed-loop pole constraint.

$$\Pi_{cl}=\{\chi_i=-a_i+j\bar{\omega}_{di} | (a_i, \bar{\omega}_{di}) \in \Re, (\alpha, \beta, r) \in \Re, i=1, 2, \cdots, n\} \text{ with } j=\sqrt{-1}$$

where $\bar{\omega}_{di}$ is a damped natural frequency. It is well known that the pole constraint directly impacts many dynamic characteristics of the closed-loop system (that is, rise time, settling time, and maximum overshoot, etc.). The convex regions Π_{cl} can be given as LMI via the Lyapunov matrix X_Π.

Theorem 1: There exists a state feedback gain $K_\Pi (\in k)$ such that all poles of the closed-loop system Σ_{cl} are located in the prescribed LMI region of the manifold:

$$\Pi_{cl}=\{\chi \in C : \Phi(\chi, \bar{\chi}) < 0\} \tag{13}$$

where the Hermitian matrix Φ is given by $\Phi(\chi, \bar{\chi}) = E+N\chi+N^T\bar{\chi}$ with the fixed matrices $E=E^T$ and N, if and if only there exists a matrix $X_\Pi = X_\Pi^T > 0$ which satisfies the following inequality:

$$[\lambda_{ij} X_\Pi + \varepsilon_{ij} A_c X_\Pi + \varepsilon_{ij} X_\Pi A_c^T]_{i,j=1}^m < 0 \tag{14}$$

where $[\lambda_{ij}]_{i,j=1}^m$ and $[\varepsilon_{ij}]_{i,j=1}^m$ are the generic entries of the Hermitian matrices $V \in C^{(m\times m)}$ and $N \in C^{(m\times m)}$, respectively.

Proof: See Wang et al. (1995), and Chilali and Gahinet (1996). ■ ■

If all eigenvalues of A_{cl} are confined to the desired domain Π_{cl}, the vehicle system modes damp asymptotically at desired rates and achieve a specified degree of stability.

3.3 H_∞ optimal compensator design

The H_∞ suboptimal task is to design a control-

ler $K_\infty(\in k)$ which stabilizes the generalized vehicle model. The closed-loop L_2-induced norm constraint is formalized as $\|T_{z_\infty w}\|_\infty = \sup_\omega \|T_{z_\infty w}(j\bar{\omega})\|_\infty < \gamma_\infty$ for a given $\gamma_\infty \in \Re^+$, where L_2 is the square-integrable signals defined over R^+. Based on the Bounded Real Lemma (Iwasaki and Skelton, 1994), the H_∞ suboptimal synthesis can be expressed in the following LMIs (Boyd *et al.*, 1994; Khargonekar and Rotea, 1991; Niewoehner and Kaminer, 1996).

Theorem 2: For the given plant P, there exists a controller K_∞ that satisfies the H_∞ suboptimal constraint γ_∞ with the internal stability of $T_{z_\infty w}$ in Eq. (11) (or $\sum_{cl\infty}$) if and if only there exist a Lyapunov matrix $X_\infty > 0$ satisfying the following LMI:

$$\begin{pmatrix} A_{cl}X_\infty + X_\infty A_{cl}^T & B_{cl} & X_\infty C_{cl\infty}^T \\ B_{cl}^T & -\gamma_\infty I & D_{cl\infty}^T \\ C_{cl\infty}X_\infty & D_{lc\infty} & -\gamma_\infty I \end{pmatrix} < 0 \qquad (15)$$

Proof: See You (1997) for the complete proof. ■

■

It follows that the L_2 norm gain of the input/output mapping between w and z_∞ is clearly bounded as $\|z_\infty\|_2 < \gamma_\infty \|w\|_2$. Further, a pure H_∞ optimal problem with a gain matrix $K_{\infty opt}(\in k)$ can be obtained such that $\inf_{K\infty opt} \|T_{z_\infty w}\|_\infty = \gamma_{\infty opt}$, where $\gamma_{\infty opt}$ is a minimal attainable scalar number.

3.4 H_2 optimal compensator design

The H_2 optimal synthesis is to seek to minimize $\|T_{z_2 w}\|$ (in $\sum_{cl2}$) with a gain matrix $K_{2opt}(\in k)$. First, the H_2 norm of the system satisfies the following constraint with $D_{21}=0$:

$$\|T_{z_2 w}\|_2^2 = Trace(C_{cl2} X C_{cl2}^T) < \infty \qquad (16)$$

where $X > 0$ is the controllability Gramian of (A_{cl}, B_{cl}). We also obtain the following Lyapunov equation:

$$A_{cl}X + XA_{cl}^T + B_{cl}B_{cl}^T = 0 \qquad (17)$$

Let $X_2 (> X)$ denote a positive-definite solution to the following Lyapunov inequality:

$$A_{cl}X_2 + X_2 A_{cl}^T + B_{cl}B_{cl}^T < 0 \qquad (18)$$

it follows that

$$\|T_{z_2 w}\|_2^2 < Trace(C_{cl2} X_2 C_{cl2}^T \qquad (19)$$

Furthermore, the matrices $X_2 = X_2^T$ and $R = R^T$ satisfy the following LMIs:

$$\begin{pmatrix} A_{cl}X_2 + X_2 A_{cl}^T & B_{cl} \\ B_{cl}^T & -I \end{pmatrix} < 0 \qquad (20)$$

$$\begin{pmatrix} R & C_{cl2}X_2 \\ X_2 C_{cl2}^T & X_2 \end{pmatrix} > 0 \qquad (21)$$

Then it is readily shown to be as $\|T_{z_2 w}\|_2^2 < Trace(R)$. Now, it is straightforward to show the following theorem.

Theorem 3: For the given plant P, there exists a stabilizing feedback gain K_{2opt} such that the closed-loop norm $\|T_{z_2 w}\|_2$ is minimized if and if only there exists two symmetric matrices $X_2 = X_2^T$ and $R = R^T$ satisfying a set of LMIs (20) and (21).

Proof: The proof of the theorem is given above. ■

■

It is readily shown that $\|T_{z_2 w}\|_2$ is the minimum of $\sqrt{Trace(R)}$ subject to a set of LMIs given in (20) and (21). Further, there exists a scalar $\gamma_2 \in \Re^+$ such that $\sqrt{Trace(R)} \le \gamma_2$. Clearly, the H_2 norm with $\|T_{z_2 w}\|_2^2 = \inf\{Trace(C_{cl2} X_2 C_{cl2}^T)\} = \gamma_{2opt}^2$ can be established with a minimal upper bound $\gamma_{2opt} \ge 0$.

3.5 Mixed H_2/H_∞ suboptimal synthesis with pole placement

In this paper, the general design objective is achieved by combining the H_2/H_∞ synthesis with the pole constraint. However, a set of matrices $(X_\infty, X_2, X_\Pi, R, K)$ simultaneously satisfying the LMIs given in (14), (15), (20) and (21) is not convex. It requires that the Lyapunov matrices in all specifications should be imposed by the constraint $X_\infty = X_2 = X_\Pi = X_C$, where X_C is a common Lyapunov matrix (Khargonekar and Roeta, 1991; Boyd et al., 1994; Iwasaki and Skelton, 1994). Then the global asymptotic stability for the closed-loop system (10) (or $\sum_{cl}$) can be established by choosing a Lyapunov function $V(t, x_{cl}) = x_{cl}^T X_C x_{cl}$ with $X_C = X_C^T > 0$. Let a new matrix Q be $Q = K_{2\infty} X_C$ with $K_{2\infty}(\in k)$. When the performance criteria γ_2 and γ_∞ are both finite, a combined solution yields a stable closed loop system that satisfies the following LMI based convex optimization problem.

Theorem 4: There exists a stabilizing state-feedback control law $\boldsymbol{u}=\boldsymbol{K}_{2\infty}\boldsymbol{x}$, which can be incorporated into the mixed H_2/H_∞ synthesis with the pole placement, if and only if there exist the matrices $X_C=X_C^T$, $\boldsymbol{Q}$, and $\boldsymbol{R}=\boldsymbol{R}^T$ such that

inf{*Trace*($\boldsymbol{R}$)} subject to a set of LMIs (14), (15), (20), and (21)

with $X_C>0$ and $\boldsymbol{Q}=\boldsymbol{K}_{2\infty}\boldsymbol{X}_C$.

Proof: Based on the above theorems (1~3), it is straightforward to show this theorem. ■ ■

Since a set of matrices ($\boldsymbol{X}_C$, $\boldsymbol{R}$, $\boldsymbol{Q}$) exist, a controller has a constant-gain matrix $\boldsymbol{K}_{2\infty}$ given by $\boldsymbol{K}_{2\infty}=\boldsymbol{Q}\boldsymbol{X}_C^{-1}$. The corresponding control law is $\boldsymbol{u}=\boldsymbol{K}_{2\infty}\boldsymbol{x}=\boldsymbol{Q}\boldsymbol{X}_C^{-1}\boldsymbol{x}$ via the matrix transformation.

4. Maneuvering Simulation Results

In diving motion control, the output variables (z_∞, z_2) of interest in (7) are respectively selected as

$$z_\infty=\begin{bmatrix}h\\ \theta\end{bmatrix}=\overbrace{\begin{bmatrix}0&0&1&0\\ 0&0&0&1\end{bmatrix}}^{C_1}\begin{bmatrix}\omega\\ q\\ h\\ \theta\end{bmatrix}$$

$$=\boldsymbol{C}_1\boldsymbol{x}+\boldsymbol{D}_{11}\boldsymbol{w}+\boldsymbol{D}_{12}\boldsymbol{u} \tag{22}$$

$$z_2=\begin{bmatrix}\omega\\ q\\ \delta_b\\ \delta_s\end{bmatrix}=\overbrace{\begin{bmatrix}1&0&0&0\\ 0&1&0&0\\ 0&0&0&0\\ 0&0&0&0\end{bmatrix}}^{\boldsymbol{C}_2}\begin{bmatrix}\omega\\ q\\ h\\ \theta\end{bmatrix}+\overbrace{\begin{bmatrix}0&0\\ 0&0\\ 1&0\\ 0&1\end{bmatrix}}^{\boldsymbol{D}_{22}}\begin{bmatrix}\delta_b\\ \delta_s\end{bmatrix}$$

$$=\boldsymbol{C}_2\boldsymbol{x}+\boldsymbol{D}_{21}\boldsymbol{w}+\boldsymbol{D}_{22}\boldsymbol{u} \tag{23}$$

where other matrices are given as $\boldsymbol{D}_{11}=\boldsymbol{0}$, $\boldsymbol{D}_{12}=\boldsymbol{0}$, and $\boldsymbol{D}_{21}=\boldsymbol{0}$. For convenience, the external disturbances are assumed to be $\boldsymbol{w}=w$ (or $w_1=w_2=w$) along with $b_1=1$ and $b_2=10$ in (5). Based on the vehicle dynamics and the control strategies described above, we present numerical simulation results to evaluate the autopilot performance.

4.1 Normalized vehicle model

With the constant forward speed (6 knots), Tables 1 and 2 describe the nominal data for a typical underwater vehicle with their physical units (Healey and Lienard, 1993).

Now, the linearized vehicle model $\sum_P$ is scaled to enhance the efficiency of numerical simulations. A set of new vehicle variables are given as:

$\tilde{\omega}=10^4\delta\omega$; $\tilde{q}=10\,\delta q$; $\tilde{h}=10^3\delta h$; $\tilde{\theta}=10^3\delta\theta$; $\tilde{\delta}_{b,s}=10^3\delta_{b,s}$; $\tilde{w}=w$.

Then we describe the normalized state-space equations for the given conditions in Table 1 and 2 by

$$\sum_{\tilde{P}}:\begin{cases}\dot{\boldsymbol{x}}=\tilde{\boldsymbol{A}}\tilde{\boldsymbol{x}}+\tilde{\boldsymbol{B}}_1\tilde{\boldsymbol{w}}+\tilde{\boldsymbol{B}}_2\tilde{\boldsymbol{u}}\\ \tilde{z}_\infty=\tilde{\boldsymbol{C}}_1\tilde{\boldsymbol{x}}+\tilde{\boldsymbol{D}}_{11}\tilde{\boldsymbol{w}}+\tilde{\boldsymbol{D}}_{12}\tilde{\boldsymbol{u}}\\ \tilde{z}_2=\tilde{\boldsymbol{C}}_2\tilde{\boldsymbol{x}}+\tilde{\boldsymbol{D}}_{21}\tilde{\boldsymbol{w}}+\tilde{\boldsymbol{D}}_{22}\tilde{\boldsymbol{u}}\end{cases} \tag{24}$$

where all the corresponding matrices are calculated in Appendix. In the following, all variables are given in the normalized forms.

4.2 Numerical simulations

To begin, we consider the open-loop system ($\sum_{\tilde{P}}$) without control law. As shown in Fig. 4, the open-loop poles are 0, −0.4370, and −0.9304 $\pm j2.8467$. We assign the closed-loop poles in the

Table 1 Vehicle model parmeters

$U=3.065$[m/sec]	$W_w=53400[N]$	$W_B=53400[N]$
$\rho=1000$[kg/m^3]	$l=5.3$[m]	$\bar{x}_G=0.0$[m]
$\bar{x}_B=0.0$[m]	$\bar{z}_G=6.1$[m]	$\bar{z}_B=0.0$[m]
$J_{\bar{y}}=13587$[kg·m^2]	$g=9.81$[m/sec^2]	

Table 2 Nondimensional hydrodynamic coefficients for the vehicle(*estimated)

$Z_{\dot{w}}=-2.4\times10^{-1}$	$Z_{\dot{q}}=-6.8\times10^{-3}$	$M_{\dot{w}}=-6.8\times10^{-2}$	$M_{\dot{q}}=-1.7\times10^{-2}$
$Z_w=-3.0\times10^{-1}$	$Z_q=-1.4\times10^{-1}$	$M_w=1.0\times10^{-1}$	$M_q=-6.8\times10^{-2}$
$^*Z_{\delta_b}=-3.0\times10^{-2}$	$Z_{\delta_s}=-7.3\times10^{-2}$	$^*M_{\delta_b}=6.0\times10^{-3}$	$M_{\delta_s}=-4.1\times10^{-2}$

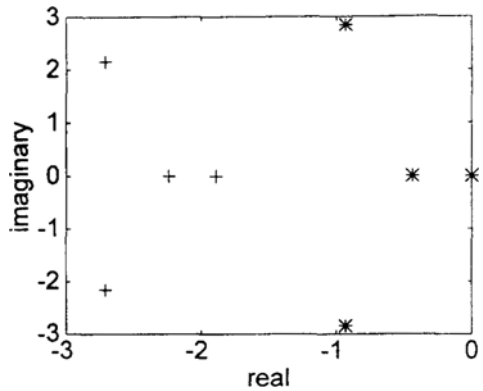

Fig. 4 Pole placement plots: open-loop(*), closed-loop(+).

specified region $\Pi_{cl}(-1.7, \pi/4, 20)$ of a stable complex plane to obtain well-damped transient responses. Unless mentioned otherwise, all pertinent parameters as well as pole constraint are identical in the closed-loop simulations. In diving autopilot design, the control engineer is required to guarantee an acceptable level of disturbance attenuation ($\gamma_\infty = 1$) while keeping the control effort acceptably low: minimization of the H_2 norm of $T_{\tilde{z}_2\tilde{w}}$ subject to $\|T_{\tilde{z}_\infty\tilde{w}}\|_\infty < 1$ (or 0 dB) with pole constraint Π_{cl}. Now, the actual closed-loop poles are placed at -2.2387, -1.8890, and $-2.7085 \pm j2.158$, which obviously satisfy the pole constraints (see Fig. 4). The resulting state-feedback law with $\tilde{x} \in \Re^4$ is given by $\tilde{u}(t) = K\tilde{x}(t)$, where the control gain matrix is

$$K_{2\infty} = \begin{bmatrix} 0.7794 & -5.1960 & 6.2846 & -11.4157 \\ 0.1248 & 0.7523 & -1.1202 & 2.2992 \end{bmatrix}.$$

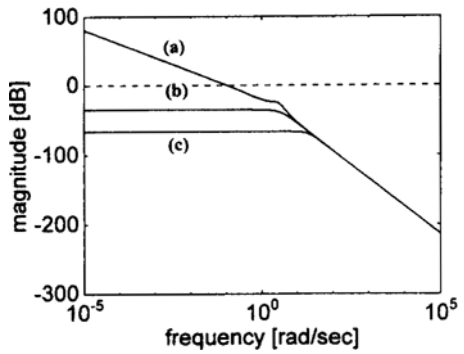

Fig. 5 Singular value plots between impulse input w and z_∞ for: (a) open-loop, (b) mixed H_2/H_∞ synthesis with pole constraints, (c) H_∞-optimal

In robust control theory singular values have been used to extend the classical frequency response Bode plot to MIMO systems. The singular value plots of the open-loop vs closed-loop system are shown in Fig. 5. As expected, the singular value plots for the closed-loop systems show that the disturbances are rejected very well at the low frequencies (≤ 0 dB). Furthermore, the noise attenuation (or suppression) is reasonable at high-frequencies (roll-off rate $\leq$ 40dB/decade). In addition, for the given values $\gamma_\infty = 1$ and $\gamma_{2opt} = 0.981$, we evaluate the time responses of the closed-loop system for the impulse-type disturbances in Figs 6 and 7 along with control input activities (Fig. 8). For the comparison purpose, we present the following results: the smaller the infinity norm γ_∞, the better the system is able to reject disturbances. We can also decrease the attenuation level $\gamma_\infty (\gamma_\infty > \gamma_{\infty opt})$ at expense of a minimum gain γ_{2opt} in H_2/H_∞ method. Further, the best performance level $\gamma_{\infty opt}$ that can be obtained for H_∞ alone (or H_∞-optimal) is $\gamma_{\infty opt} \approx 4.85 \times 10^{-4}$ (see Fig. 5) with high control gain:

$$K_{\infty opt} = 10^3 \times \begin{bmatrix} 0.0118 & -0.0172 & 1.2954 & -0.3690 \\ 0.0023 & 0.0057 & 0.2491 & 0.0579 \end{bmatrix}.$$

All simulation results show that the design objectives are certainly achieved. As stated in Sec3, we present various control approaches (H_2, H_∞, mixed H_2/H_∞ with pole assignment) via LMIs. Based on the control objective of a given system, one can choose an appropriate control scheme to

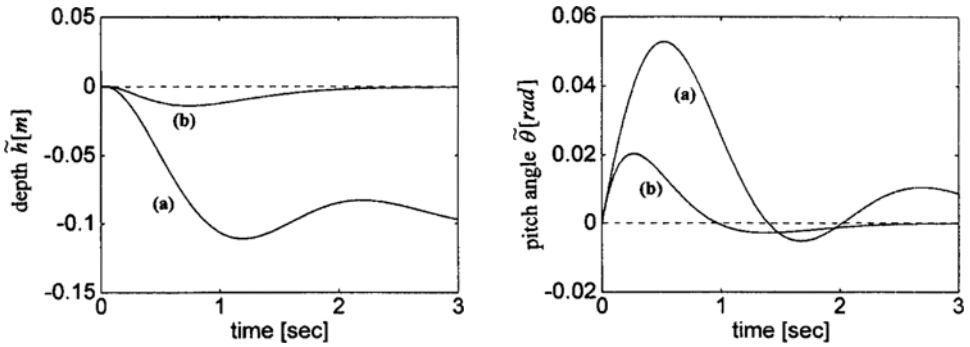

Fig. 6 Time responses of output variables z_∞ to impulse disturbance w: (a) open-loop, (b) mixed H_2/H_∞ synthesis with pole constraints.

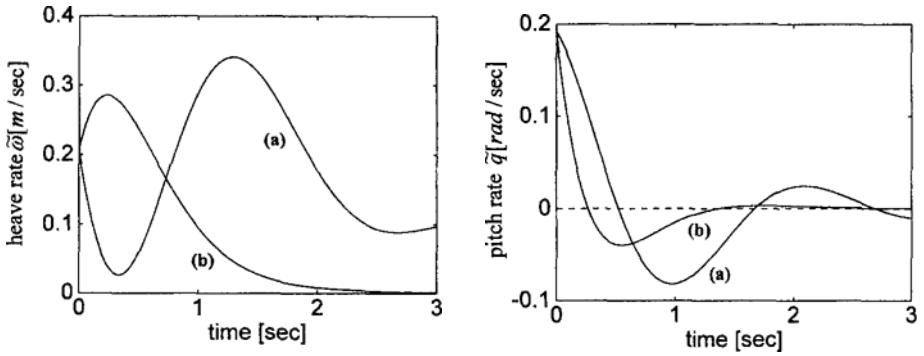

Fig. 7 Time responses of output variables z_2 to impulse disturbance w: (a) open-loop, (b) H_2/H_∞ synthesis with pole constraints

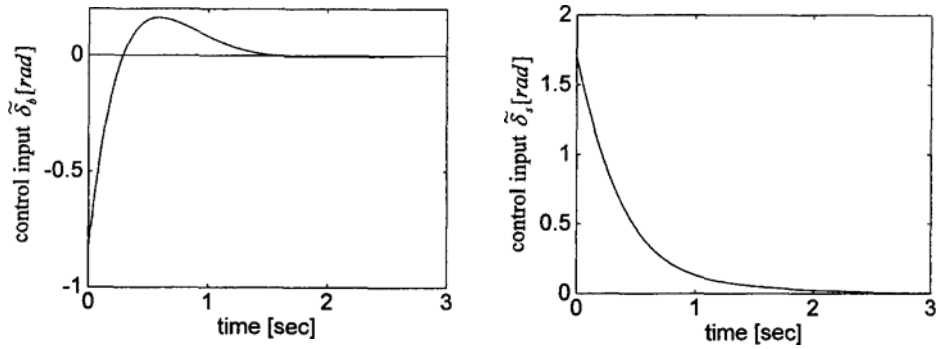

Fig. 8 Control input activities u to impulse disturbance w

obtain the desired performance. In fact, using the parameters (α, β, r, γ_∞) given in Sec 3, we can greatly improve the system performance in time-domain as well as frequency-domain.

5. Conclusions

This paper addresses the application of the robust multivariable control scheme for a submersible vehicle designed to perform a variety of missions. The first part of the paper is concerned with a compact linear model of the vehicle. Next, the mathematical models and the robust control algorithms are integrated in the diving autopilot design phase. Furthermore, we have reformulated the mixed H_2/H_∞ synthesis problem with pole constraint using LMIs. A complete simulation analysis in both the time and frequency domains is provided in order to explicitly evaluate the vehicle guidance and control performance. It has been shown that the robust controllers we have selected give excellent performance and satisfy the control magnitude limit. Finally, the LMI-based guidance and control approach provides tractable means to design the robust controller. The diving autopilot provides a multi-objective optimization solution posed by several competing objective functions and can readily manipulate the uncertain vehicle system.

References

Bernstein, D. D., Haddad, W. H., and Mustafa, D., 1991, "Mixed H_2/H_∞ Regulation and Estimation: the Discrete-Time Case," *Syst. Contr. Letters,* Vol. 16, pp. 235~247.

Boyd, S., Ghaoui, L. E., Feron, E., and Balakrishan, V., 1994, *Linear Matrix Inequalities in System and Control Theory,* SIAM, Philadelphia.

Chilali, M., and Gahinet, P., 1996, "H_∞ Design With Pole Placement Constraints: an LMI

Approach," *IEEE Trans. Auto. Contr.*, Vol. 41, pp. 358~367.

Clayton, B. R., and Bishop, R. E., 1982, Mechanics of *Marine Vehicles*, E. & F. N. Spon, London.

Doyle, J. C., Glover, K., Khargonekar, P. P., and Francis, B. A., 1989, "State-space Solutions to Standard H_2 and H_∞ Control Problems," *IEEE Trans. Auto. Contr.*, Vol. 34, pp. 831~847.

Geuler, G. F., 1989, "Modelling, Design and Analysis of an Autopilot for Submarine Vehicles," *Int. Ship. Progress*, Vol. 36, pp. 51~85.

Glover, K., and Doyle, J. C., 1988, "State Space Formula for All Stabilizing Controllers That Satisfy an H_∞ Norm Bound and Relations to Risk Sensitivity," *Syst. Contr. Letters*, Vol. 11, pp. 167~172.

Healey, A. J., and Lienard, D., 1993, "Multivariable Sliding Mode Control for Autonomous Diving and Steering of Unmanned Underwater Vehicles," *IEEE J. Ocean Engr.*, Vol. 18, pp. 327~339.

Iwasaki, I., and Skelton, R. E., 1994, "All Controllers for the General H_∞ Control Problem: LMI Existence Conditions and State Space Formulas," *Automatica*, Vol. 30, pp. 1307~317.

Khargonekar, P., and Rotea, M., 1991, "Mixed H_2/H_∞ Control: a Convex Optimization Approach," *IEEE Trans. Auto. Contr.*, Vol. 36, pp. 824~836.

Marshfield, W. B., 1991, "Submarine Periscope -Depth Depth-Keeping Using an H-Infinity Controller Together with Sea-Noise-Reduction Notch Filters," *Trans. Institute Meas. Contr.*, Vol. 13, pp. 233~240.

Niewoehner, R. J., and Kaminer, I. I., 1996, "Integrated Aircraft-Controller Design Using Linear Matrix Inequalities," *AIAA J. Guid. Contr. Dynamics*, Vol. 19, pp. 445~452.

Papoulias, F. A., 1993, "Dynamics and Bifurcations of Pursuit Guidance for Vehicle Path Keeping in the Dive Plane," *J. Ship Research*, Vol. 37, pp. 148~165.

You, S. S., and Jeong, S. K., 1996, "Model -Based Feedforward Precompensation and VS-Type Robust Nonlinear Controller Postcompensation for Uncertain Robotic Systems with/Without Knowledge of Uncertainty Bounds," *KSME Journal*, Vol. 10, pp. 296~304.

You, S. S., 1997, "Robust Autopilot Design for Submarine Vehicles," *J. Ocean Engr. Tech.*, Vol. 10, pp. 180~190.

Wang, Z., Chen, X., and Guo, Z., 1995, "Controller Design for Continuous Systems with Variance and Circular Pole Constraints," *Int. J. System Science*, Vol. 26, pp. 1249~1256.

Appendix

All system matrices in normalized state-space model (24) are clearly defined here:

$$\tilde{A}=\begin{bmatrix} -0.8935 & -4.9294 & 0 & 8.1423 \\ 0.2949 & -1.4044 & 0 & -7.0743 \\ 0.1 & 0 & 0 & -3.0650 \\ 0 & 1 & 0 & 0 \end{bmatrix},$$

$$\tilde{B}_1=\begin{bmatrix} 0.2078 \\ 0.1922 \\ 0 \\ 0 \end{bmatrix},\quad \tilde{B}_2=\begin{bmatrix} -2.3679 & -0.6110 \\ 0.5819 & -3.0593 \\ 0 & 0 \\ 0 & 0 \end{bmatrix}$$

$$\tilde{C}_1=\begin{bmatrix} 0 & 0 & 1 & 0 \\ 0 & 0 & 0 & 1 \end{bmatrix},\quad \tilde{C}_2=\begin{bmatrix} 1 & 0 & 0 & 0 \\ 0 & 1 & 0 & 0 \\ 0 & 0 & 0 & 0 \\ 0 & 0 & 0 & 0 \end{bmatrix},$$

$$\tilde{D}_{22}=\begin{bmatrix} 0 & 0 \\ 0 & 0 \\ 1 & 0 \\ 0 & 10 \end{bmatrix},\quad \tilde{D}_{11}=\mathbf{0}_{2\times 1},\ \tilde{D}_{12}=\mathbf{0}_{2\times 2},\ \tilde{D}_{21}=\mathbf{0}_{4\times 1}.$$